

# On the scientific utilisation of low power research reactors

P. Mikula<sup>1</sup>, P. Strunz<sup>1</sup>

<sup>1</sup>Nuclear Physics Institute ASCR, v.v.i. 25068 Řež, Czech Republic

*E-mail contact of main author: mikula@ujf.cas.cz*

**Abstract.** In our contribution we focus our attention on the scientific utilisation of the beam tubes at the low power research reactor LVR-15. Namely, it will be reported about the neutron scattering instrumentation development and the educational possibilities at the low power neutron sources. The feasibility of carrying out the methodology and instrumental development research at the low power neutron sources will be demonstrated on designs of several high resolution and good luminosity neutron scattering instruments exploiting Bragg diffraction optics. Some of them have been already realized e.g. for small angle neutron scattering studies or residual strain/stress measurements. As the mentioned instrumental development and testing can be carried out at the low power neutron sources, due to the much lower safety requirements in comparison with the medium and high flux sources, they offer excellent educational and training programmes in neutron scattering or imaging for students.

**Key Words:** Low power reactor, research with thermal neutrons

## 1. Introduction

The present reactor LVR-15 was originally introduced in the operation in 1957 at 2 MW power. Later on, after two reconstructions the present tank type light water reactor has used the uranium fuel enriched to 36 and finally 20 percent in uranium-235 and can operate at any power up to the licensed ceiling of 10 MW. It operates on average about 170 days per year with a pattern of operating cycles of three weeks plus one week for maintenance and instrumentation development. The thermal neutron flux in the core is the most of about  $9 \times 10^{13}$

TABLE I: Reactor parameters

Mean reactor power	10 MW
Maximum thermal neutron flux in the core	Max $1 \cdot 10^{18} \text{ n} \cdot \text{m}^{-2} \cdot \text{s}^{-1}$
Maximum fast neutrons flux in the core	$3 \cdot 10^{18} \text{ n} \cdot \text{m}^{-2} \cdot \text{s}^{-1}$
Maximum thermal flux in reflector (mix of Be + H <sub>2</sub> O)	$5 \cdot 10^{17} \text{ n} \cdot \text{m}^{-2} \cdot \text{s}^{-1}$
Maximum thermal neutron flux in the tubes	$1 \cdot 10^{12} \text{ n} \cdot \text{m}^{-2} \cdot \text{s}^{-1}$
Maximum thermal flux at the exit of the tubes (100/60 mm)	$1 \cdot 10^8 \text{ n} \cdot \text{m}^{-2} \cdot \text{s}^{-1}$
Irradiation channel - in fuel	Max. $1 \cdot 10^{14} \text{ n} \cdot \text{m}^{-2} \cdot \text{s}^{-1}$
Irradiation channel - at core periphery	$7 \cdot 10^{13} \text{ n} \cdot \text{m}^{-2} \cdot \text{s}^{-1}$
Doped silicon facility	$1 \cdot 10^{13} \text{ n} \cdot \text{m}^{-2} \cdot \text{s}^{-1}$
High pressure water loops	$5 \cdot 10^{13} \text{ n} \cdot \text{m}^{-2} \cdot \text{s}^{-1}$

$\text{n.cm}^2.\text{s}^{-1}$  (see Table 1) and can be considered as a low power reactor. At present, it belongs to the Research Centre Rez, Ltd. and is operated mainly on a commercial basis. Research and development in Research Centre Rez, Ltd. is focused on the area of nuclear energy, nuclear reactor physics, chemistry and materials. The irradiation service uses the reactor namely for: Modification of Physical Characteristics of Materials, Production of Radionuclides for Radiopharmacy and Production of Radionuclide Emitters. Crucial for research and development of the reactor are technological circuits – experimental loops for modelling of experimental conditions in the reactor core and the connected reactor cooling circuits. These loops allow mechanical, thermal-hydraulic, material, corrosion and further research at parameters and under operating conditions of the reactor concept under development. By placing a loop in the experimental reactor, all the above-mentioned physical and chemical influences of reactor coolant are supplemented by radiation conditions. The results are used in services for both Czech and foreign related organizations. On the other hand, Neutron Physics Laboratory (NPL) of Nuclear Physics Institute of the Czech Academy of Sciences performs effectively neutron physics experiments when using horizontal and vertical irradiation beam channels of the reactor [1,2]. In total, NPL operates 8 instruments installed at 5 radial horizontal beam tubes (for experiments in nuclear physics, solid state physics and materials research) and two vertical irradiation channels (for neutron activation analysis) which are hired at Research Centre Rez, Ltd. A good quality of the experiments carried out at the reactor in Řež is documented by the fact that NPL laboratory participated in the EU Project - ACCESS (Transnational Access to Large Facilities) in the frame of FP7-NMI3 programme which finished in January. 2016. The following instruments are used at this low power research reactor at a good level (see Fig. 1): Two strain/stress scanners (HK4+HK9), Small-angle neutron scattering (SANS) diffractometer (HK8a), Neutron powder diffractometer MEREDIT (HK6), Thermal neutron depth profiling facility (HK3), Neutron activation analysis facility (NAA), Neutron optics diffractometer (HK8b). Effectiveness of the neutron

scattering instruments is supported by employment of neutron optics devices in combination with position sensitive detectors (PSD). The powder diffractometer installed at the horizontal channel HK2 is operated by the Faculty of Nuclear Sciences and Physical Engineering of the Czech Technical University in Prague.

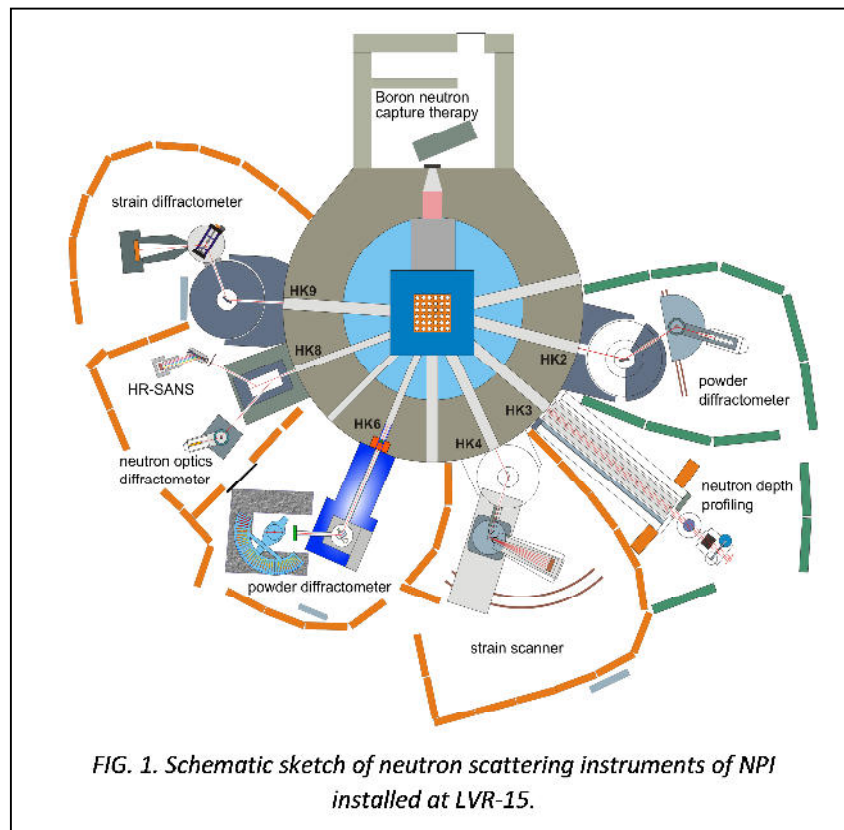
## 2. Experimental activities at the reactor LVR-15

### 2.1. Thermal neutron analytical methods

Three instruments HK3-a HK-b and HK3-c operate at the thermal neutron beam formed by short neutron guide tube. The neutron guide ensures an efficient transport of thermal neutrons from a  $\phi=100$  mm horizontal channel of the reactor to small target areas of the HK3-a, HK3-b and HK3-c spectrometers. The neutron guide is built of a mirror type tube of rectangular cross-section, cylindrically bent in the vertical direction. It consists of 15 mirror sections made of glass plates of float type. The surface of these plates is coated with Ni reflecting layer with thickness of 2000 Å. The internal cross-section of each mirror section is  $4 \times 150$  mm<sup>2</sup>. The overall length of the guide is 5.63 m, the curvature radius being 825 m. In order to suppress a background due to a direct beam of gamma rays and fast neutrons, the guide is tightly surrounded by a combined shielding consisting of lead and polyethylene pellets. Unlike thermal neutrons, gamma rays and fast neutrons are not subject to reflections from the Ni coating and penetrate the guide walls. In the shielding around they are scattered and absorbed and only collimated thermal neutrons pass through. In addition, a biological shielding, formed by boron-doped polyethylene and lead bricks, is built along the whole guide. The shape of the incoming neutron beam at the entrance of the guide matches the cross-section of the guide. This has been achieved using a 90 cm long collimator made of lead with a rectangular aperture. Immediately behind the guide exit, the neutron beam is tailored by an additional collimator made of <sup>6</sup>Li<sub>2</sub>CO<sub>3</sub> to reduce the beam cross-section to  $4 \times 60$  mm<sup>2</sup>.

The flux thermal at the exit over the cross-section is

of neutrons guide averaged beam section



$(1.5 \pm 0.2) \cdot 10^7 \text{ n cm}^{-2} \text{ s}^{-1}$ . The cadmium ratio is equal approximately to  $10^5$ . The above mentioned fluxes refer to the reactor power of 8 MW. Beyond the guide exit, the vertical divergence of neutron trajectories is characterized by angular deviations below  $0.5^\circ$ .

### **2.1.1. Neutron depth profiling (NDP)**

NDP facility was set up just behind the neutron guide at HK3. The multidetector spectrometer consists of a large vacuum chamber, automatic target holders and several different data acquisition systems which can be used at the same time. NDP is the nuclear analytical

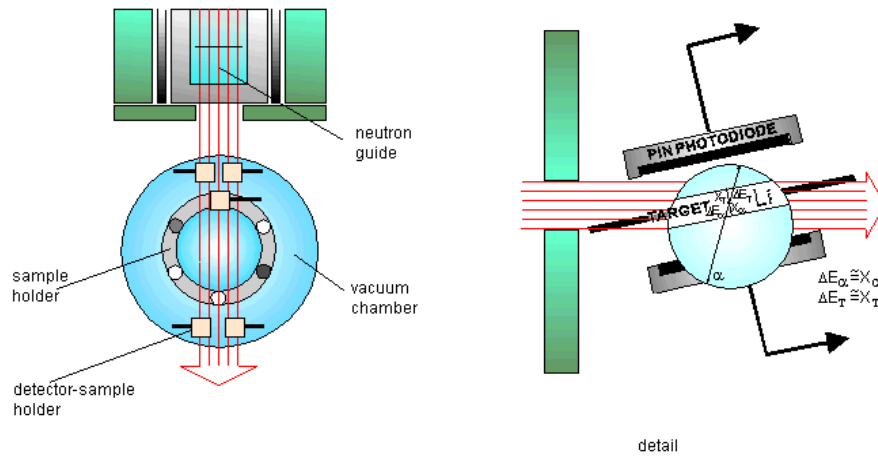


FIG. 2. Schematic sketch of the NDP facility

technique available to profile light elements in solids. It utilizes the existence of isotopes of elements that produce prompt monoenergetic charged particles upon capture of thermal neutrons. From the energy loss spectra of emitted products the depth distributions of light elements can be reconstructed. The NDP method is an excellent tool for studies of numerous problems in solid-state physics (diffusion, sputtering), material science (corrosion), electronics, optronics, life sciences etc. Its applicability and efficiency has steadily expanded. NDP is the nuclear analytical technique available to determine depth profiles of light elements in solids (i.e.,  $^3\text{He}$ ,  $^6\text{Li}$ ,  $^{10}\text{B}$ ,  $^{14}\text{N}$ , etc.). The related multidetector spectrometer consists of a large vacuum chamber, automatic target holders and several different data acquisition systems which can be used at the same time (see Fig 2). This method uses the following parameters of the neutron beam: cross section - the height 4 mm and the width up to 90 mm, intensity of the thermal neutron beam -  $10^7 \text{ cm}^{-2}\text{s}^{-1}$ , Cd ratio -  $10^5$ , collimation - in the vertical plane  $\sim 1^\circ$  and in the horizontal plane  $\sim 1^\circ$ , beam homogeneity - inhomogeneous due to girland and zig-zag reflections. The list of the isotopes which can be used in the NDP method is shown in Table II. Fig. 3 shows also an example of the depth profiling of Boron in  $\text{CaF}_2$  as implanted and

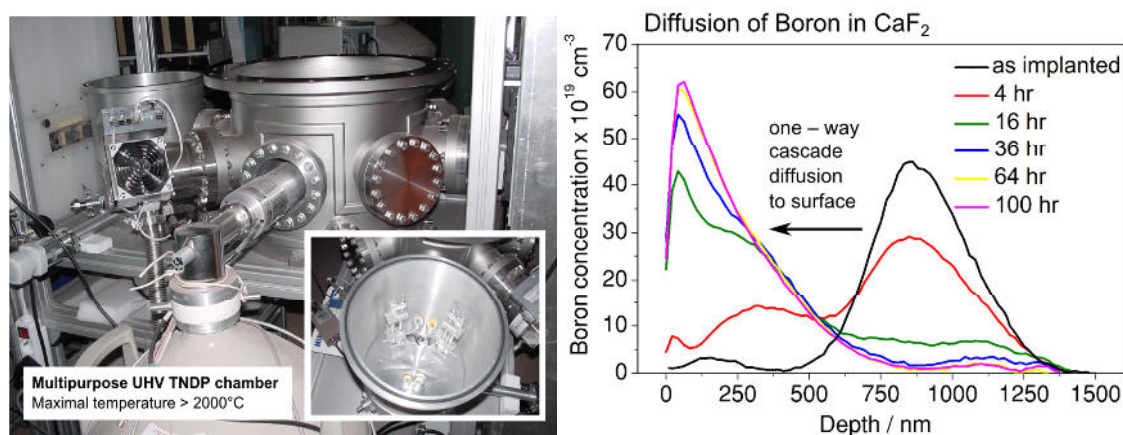


FIG. 3. Photo of the experimental chamber used for the NDP technique and an example of the depth profiling of Boron in  $\text{CaF}_2$  as implanted ( $390 \text{ keV B}$ ,  $10^{16} \text{ at. cm}^{-2}$ ) and annealed at  $600^\circ\text{C}$ .

TABLE II - List of the NDP relevant isotopes

Nuclide	Natural abundance or activity* [ at/mCi ]	Nuclear reaction	Cross section [ barn ]	Energy of reaction products [ keV ]		Detection limit [ at/cm <sup>2</sup> ]
$^3\text{He}$	$0.13 \times 10^{-3}$	$^3\text{He}(n,p)^3\text{H}$	5326	573	191	$3.1 \times 10^{13}$
$^6\text{Li}$	7.42	$^6\text{Li}(n,\alpha)^3\text{H}$	940	2051	2734	$1.8 \times 10^{14}$
$^7\text{Be}^*$	$2.5 \times 10^{14}$	$^7\text{Be}(n,p)^7\text{Li}$	48000	1438	207	$3.5 \times 10^{12}$
$^{10}\text{B}$	19.6	$^{10}\text{B}(n,\gamma\alpha)^7\text{Li}$	3606	1471	839	$4.3 \times 10^{13}$
$^{10}\text{B}$	19.6	$^{10}\text{B}(n,\alpha)^7\text{Li}$	230	1775	1014	$6.7 \times 10^{14}$
$^{14}\text{N}$	99.64	$^{14}\text{N}(n,p)^{14}\text{C}$	1.81	584	42	$9.1 \times 10^{16}$
$^{22}\text{Na}^*$	$4.4 \times 10^{15}$	$^{22}\text{Na}(n,p)^{22}\text{Ne}$	31000	2247	103	$4.7 \times 10^{12}$
$^{35}\text{S}$	0.76	$^{35}\text{S}(n,\alpha)^{30}\text{Si}$	0.14	3091	412	$1.2 \times 10^{18}$
$^{35}\text{Cl}$	75.5	$^{35}\text{Cl}(n,p)^{35}\text{S}$	0.49	598	17	$3.4 \times 10^{17}$
$^{59}\text{Ni}^*$	$1.3 \times 10^{20}$	$^{59}\text{Ni}(n,\alpha)^{56}\text{Fe}$	12.3	4757	340	$1.4 \times 10^{16}$

List of the NDP relevant isotopes - detection limits are based on the charged particle counting rate  $0.01 \text{ s}^{-1}$ , detector-sample solid angle  $0.03 \text{ Sr}$ , and intensity of the neutron beam  $\Phi_n = 10^7 \text{ cm}^{-2}\text{s}^{-1}$ .

after an annealing [3]. In general, NDP is a non-destructive method that leaves only trace amount of residual radioactivity, and examined samples can thus be measured repeatedly. Concentrations down to a ppm (with a 1D mode) or even ppb (with a 2D mode) level can be determined, depending on the element and the matrix. Profiling to depths of about 15  $\mu\text{m}$  (e.g. Li in metals) or even 60  $\mu\text{m}$  (Li in polymers) can be obtained, with a depth resolution to a few nanometers only (for glancing angle geometry). The examined samples have to be solid (or liquid with very low volatility), flat with a smooth surface (with roughness of few nm only) and minimum area of at least a few  $\text{mm}^2$ . Depending on the nuclides and the used substrates the analysis takes a few tens of minutes to a few tens of hours. The NDP technique is applicable only to the elements with a relevant cross-sections and energy of reactions [4].

### ***Instrument parameters***

<b>Beam cross-section</b>	4 x 60 mm
<b>Neutron flux</b>	$1 \cdot 10^7 \text{ n/cm}^2\text{s}$
<b>Sample size</b>	50 - 1000 $\text{mm}^2$
<b>Detector systems:</b>	
- <b>standard arrangement</b> (single detector facing the sample)	4
- <b>sandwich arrangement</b> large angle coincidence spectroscopy (2-dimensional data processing)	1
- <b>dE-E telescope arrangement</b>	1
- <b>pulse shape discrimination analysis</b>	2
<b>Solid angle of the detector-sample system</b>	0.001% - 0.1%
<b>Detectors</b>	PIN photodiode - HAMAMATSU Charged particle detector -CANBERRA
<b>Detector areas</b>	50 - 300 $\text{mm}^2$
<b>Depletion depth</b>	10 - 100 $\mu\text{m}$
<b>Detection limit</b>	
- <i>standard arrangement</i> - N, Cl	$10^{-3} \%$ at.
- He, Li, B	$10^{-5} \%$ at.
- <i>sandwich arrangement</i> - Li, B	$10^{-8} \%$ at.
<b>Depth resolution</b>	10 - 50 nm
<b>Maximum detectable depth interval</b>	3 - 70 $\mu\text{m}$

### **2.1.2. Neutron gamma activation analysis**

The facility for the measurements of  $^{10}\text{B}$  concentrations in biological samples includes HPGe detector with 25% relative efficiency and associated Pb -  $^6\text{Li}_2\text{CO}_3$  shielding. Described facility is installed at the distance of 1 m from the exit of the neutron guide. At the target position the neutron flux is approximately  $3 \times 10^6 \text{ n} \cdot \text{cm}^{-2} \text{ s}^{-1}$  at the reactor power of 8 MW. This facility makes it possible to determine  $^{10}\text{B}$  concentration of 1 ppm in 1 ml samples with a statistical uncertainty of 5% within 15 min. This instrument is in a common property with Nuclear Research Institute, plc.

### Applications:

The experimental set-up was mainly developed for the on-line determination of  $^{10}\text{B}$  concentrations of ppm-order in biological samples (see Table III). This facility can also be used for determination of other isotopes with a sufficiently large  $(n,\gamma)$  cross-section.

### Instrument parameters

Neutron flux  $3 \cdot 10^6 \text{ n/cm}^{-2} \text{ s}^{-1}$   
 Beam cross-section at target position  $25 \times 5 \text{ mm}^2$

Table III - Expected interference-free detection limit for PGAA instrument

Element	Det. limit ( $\mu\text{g}$ )	$E_\gamma$ (keV)	Element	Det. limit ( $\mu\text{g}$ )	$E_\gamma$ (keV)
Hydrogen	20	2223	Cobalt	20	230, 556
Boron	0.06	478	Nickel	200	283, 465
Nitrogen	4000	1885, 5298	Copper	10	159, 278
Sodium	70	472, 869	Zinc	700	115, 1077
Magnesium	2000	585, 1809	Selenium	40	239
Aluminium	500	1779, 7724	Molybdenum	150	720, 778
Phosphorus	2000	637, 1072	Silver	30	192, 236
Sulfur	300	840, 2379	Cadmium	0.1	559, 651
Chlorine	10	517, 786	Samarium	0.03	333, 439
Potassium	100	770, 7771	Gadolinium	0.02	182, 1186
Calcium	600	519, 1943	Gold	30	215
Titanium	40	342, 1381	Mercury	1.5	368
Chromium	150	749, 834	Lead	40000	7368
Manganese	30	847, 1811	Neodymium	10	619, 697
Iron	300	352, 7631	Indium	5	162, 186

### Application example: The determination of boron concentration in graphene powder.

Electronic properties of graphene can be changed by doping with electron-donating (nitrogen, phosphorus) or electron-withdrawing (boron) groups. Level of doping (concentration of doped group) is crucial for tuning the electrochemistry performance of graphene. Boron-doped were prepared by thermal exfoliation of graphite oxide in an atmosphere with boron trifluoride diethyl etherate at high temperatures. In this case the effect of exfoliation temperature as well as of hydrogen content in atmosphere were investigated.

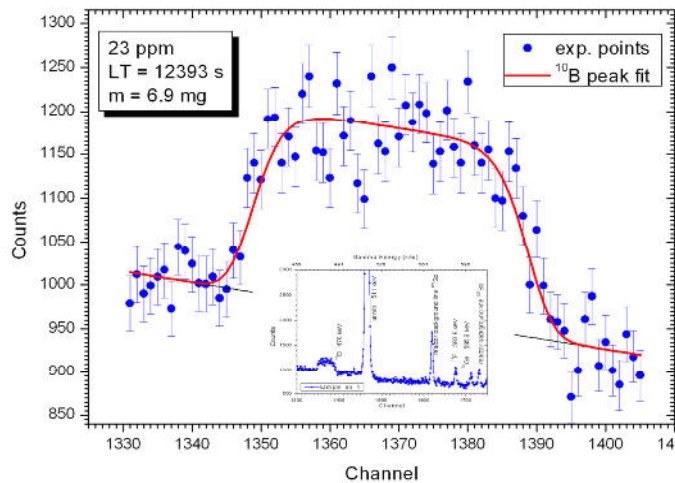


FIG. 4. Example of Doppler-broadened boron peak at 478 keV in gamma spectrum of graphene powder.

### 2.1.3. Neutron activation



**analysis (NAA)**

Both short and long time irradiation for NAA can be carried out in vertical channels H1, H5, H6 and H8 of the LVR-15 reactor (see Fig. 5). Neutron fluence rates available in these channels is given in Table IV. For the short-time NAA the channel H1 is connected with the laboratory by a pneumatic system with the transport time of 3.5 s. Irradiation is carried out in a polyethylene (PE) rabbit for 10-180 s. The channels H5, H6 and H8 are used for long-time irradiation (0.5 h – several days) in 100-mm long Al-cans. In channels H5 and H8 “narrow” (inner diameter 35 mm) Al-cans are used, which accommodate up to 35 samples packed in disk shaped PE capsules, in channel H6 “broad” (inner diameter 56 mm) Al cans are used, which accommodate up to 15 quartz vials with a 8 mm outer diameter. For epithermal neutron activation analysis (ENAA) both short- and long-time irradiation are performed behind a 1-mm Cd shielding allowing for selective activation with epithermal neutrons. The laboratory is equipped with several high resolution and high efficiency HPGe coaxial detectors. Both relative and  $k_0$  - standardization can be used for quantification of results as well as conventional  $\gamma$ -ray spectrometry. The NAA methods provide a large variety of applications: Investigations of environmental and historical materials (determination of up to 40 elements in aerosol, fly ash, soil, sediment, etc., samples by a combination of instrumental neutron activation analysis (INAA) and ENAA) [5], geo- and cosmo-chemical samples (elemental characterization of rocks, tektites, namely moldavites, and meteorites by a combination of INAA, ENAA, and radiochemical neutron activation analysis (RNAA)), in biomedicine (determination of essential and toxic trace elements in selected human and animal tissues by a combination of INAA and RNAA to achieve the lowest element detection limits possible), in forensic science (determination of poisonous elements in selected tissues of investigated cases of contemporary and historical persons) and in chemical metrology [6] (certification of element contents in reference materials prepared by the most important producers, such as U.S. NIST, IRMM, IAEA, etc.). From the recent NAA investigations, let us introduce several of them. INAA was used to determine contents of more than 30 elements in meteorites

TABLE IV - neutron fluence rates in channels for NAA irradiation at the reactor LVR-15

Channel	H1	H5	H6	H8
Energy	Fluence rate / n.cm <sup>-2</sup> .s <sup>-1</sup>			
(0.0 - 0.501 eV)	3.38E+13	6.95E+13	5.98E+13	4.02E+13
(0.031 eV - 10 keV)	1.48E+13	7.89E+13	6.89E+13	7.80E+13
(10 keV - 0.1 MeV)	3.50E+12	2.12E+13	1.78E+13	1.81E+13
(0.1 MeV - 20 MeV)	1.08E+13	5.87E+13	7.16E+13	6.27E+13

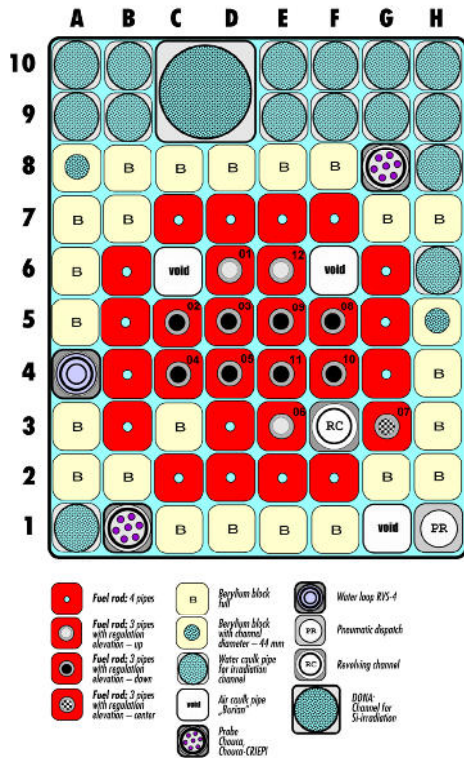


FIG. 5. LVR-15 active core layout.

in the range of  $13.7 - 44.2 \text{ mg} \cdot \text{L}^{-1}$  [12]. Concerning the cultural heritage, in 2010, the grave of the famous astronomer Tycho Brahe was opened by a Czech–Danish research consortium and samples of his bones, hair, and teeth were procured for scientific investigation. We carried out mercury determination in segmented hair samples by RNAA. The results showed that in the last 2 months of Brahe's life, he was not exposed to lethal (or fatal) doses of mercury, as was previously speculated [13]. Furthermore, graphene is another example of a material difficult to assay by classical analytical techniques. Therefore, elemental impurities were determined by INAA in graphene samples prepared by various oxidation procedures of graphite to graphite oxide followed by various reduction processes [14]. On the corresponding website one can find many other NAA results usually taken in international collaboration.

### 2.3. Neutron powder diffraction

The medium resolution powder diffractometer (MEREDIT) installed at the beam channel HK6 consists basically of consists of two large HUBER goniometer circles. It is equipped with 3 changeable monochromators placed in a massive shielding, and a multi-detector bank which is mounted in a moulded neutron shielding made from boron carbide powder in epoxy

TABLE V - monochromators and beam parameters

Monochromator	Reflection	Wavelength Å	Minimum $\Delta d/d$ ( $\times 10^{-3}$ )	Neutron flux $\text{n} \cdot \text{cm}^{-2} \cdot \text{s}^{-1}$	Beam size $\text{cm}^2$
3 bent Si single crystals	(422)	1.271	3.9 (at $56^\circ 2\theta$ )	$\sim 3.8 \times 10^9$	$2 \times 4$
	(311)	1.877	4.4 (at $58^\circ 2\theta$ )	$\sim 2.8 \times 10^9$	$2 \times 4$
3 bent Cu crystals	(220)	1.460	4.8 (at $77^\circ 2\theta$ )	$\sim 1.2 \times 10^9$	$4 \times 4$

Morávka [7] and Jesenice [8]. Environmental research was focused on the determination of  $^{129}\text{I}$  and the  $^{129}\text{I}/^{127}\text{I}$  ratio in biomonitors, namely, in bovine thyroid and moss, collected in the vicinity of the Temelin nuclear power plant (NPP) in south Bohemia using NAA in several modes (NAA with pre-irradiation separation followed by RNAA, and ENAA). No significant differences of  $^{129}\text{I}$  levels and the  $^{129}\text{I}/^{127}\text{I}$  ratios in the thyroids collected prior to the start and after several years of the NPP operation have been indicated [9]. For agricultural and nutritional research, we used a RNAA procedure to study the Se-transfer from soil or seed to wheat plants [10] and the ability of bread and durum wheat to accumulate Se via a soil-addition procedure at sowing time [11] to increase the desired uptake of the element in the Portuguese population. Silicon is an important trace element in humans, because it reduces the absorption of aluminum in human gastrointestinal tract. The daily intake of silicon should be about 10–25 mg, and its most readily absorbable form is  $\text{H}_4\text{SiO}_4$ , which is contained in beer. Using INAA, we found that Si-concentrations in Czech lager beer(s) varied

resin. The bank contains 35  $^3\text{He}$  counters with corresponding 10' Soller collimators. The

detector bank moves on air pads, which provide together with the stepping motor smooth

positioning of this heavy loaded bank. All movable parts are driven by stepping motors and

controlled by PC. The data from 35 counters are collected using two 24-channel *Tedia* cards.

Diffraction patterns can be collected in the angular range from  $2^\circ$  to  $148^\circ$  in  $2\theta_s$  with the step



down to  $0.02^\circ$  and step delay controlled by strict time or neutron flux read by a monitor.

Monochromator and beam parameters are shown in Table V. The diffractometer is mainly

used for non destructive structure phase identification, crystalline structure determination,

magnetic structure determination, temperature dependent phase transition, quantitative multi-

phase analysis and also for in-situ internal stress-strain evolution. The following sample



View to reactor



View from reactor



Neutron view



Real view 1



Real view 2



3-stage monochromator

environments are at a disposal: close cycle cryostat for 10 K  $\rightarrow$  300 K, vacuum furnace for

300 K → 1300 K, light furnace for 300 K → 1300 K, Euler goniometer, automatic six-sample-exchanger for RT and a deformation rig. The following pictures show some views of the diffractometer. There are several sample environments to enhance the measurement ability of the instrument: vacuum furnace able to cover the measurement from the room temperature up to ~1000°C; light furnace covering the same temperature range (RT up to 1000°C) but in addition is possible to heat up the sample on different atmospheres including open air, close cycle cryostat operating from room temperature down to ~10K; sample changer - carousel - for up to six samples measured at room temperature. A special deformation rig permits in-situ measurements under uniaxial stress/pressure or fatigue cycles. For textured samples, it is also possible to mount up the

Euler goniometer. For the powder samples, vanadium containers with different diameters - 6, 10 and 13 mm are used. These containers can be used only for measurement in the carousel, vacuum furnace and the close cycle cryostat. As an application example, Fig. 6 shows diffraction spectrum serving for identification of deformation of oxygen ion conductive channels (Lanthanum silicates  $\text{La}_{9.33+x}(\text{Si}_{1-y}\text{M}_y\text{O}_4)_6\text{O}_{2+3x/2}$ ;  $\text{M} = \{\text{Fe}, \text{Al}, \text{Mg}\}$  with apatite like crystal structure with space group  $\text{P6}_3/\text{m}$  are interesting material due to the high oxygen ion conductivity for fuel cell applications) and Fig. 7 shows the result of the nondestructive phase analysis of the Roman cavalry helmet from 2<sup>nd</sup> century A.D., where phase analysis of the surface corrosion products was carried out [15] and an estimation of Zn content to be of 18 wt% in the brass material was identified.

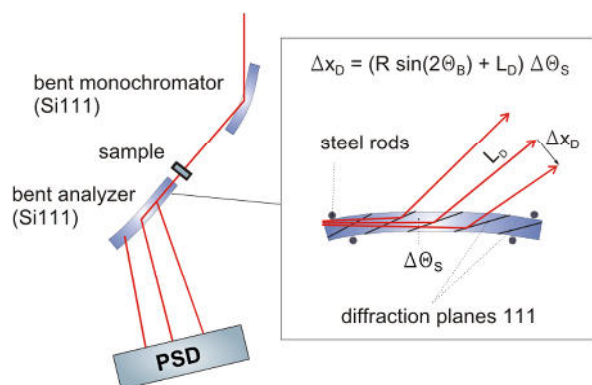
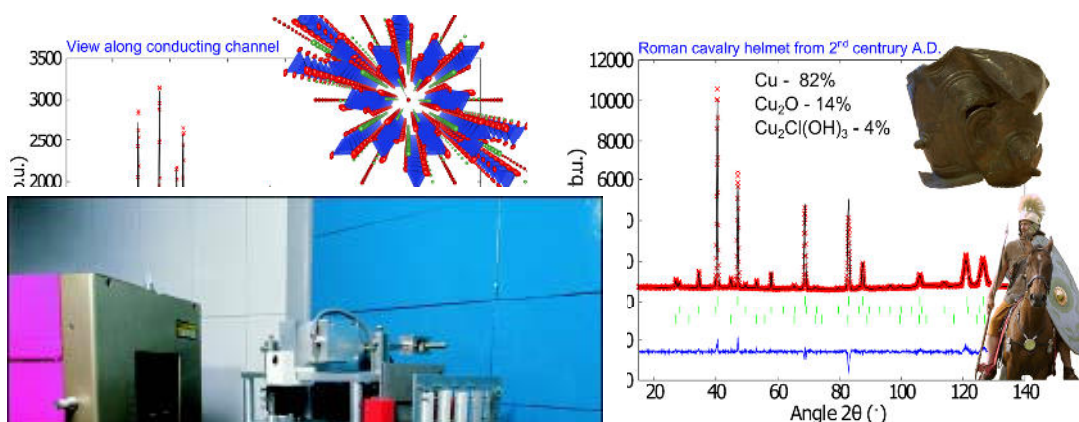


FIG. 8. Schematic sketch of the double-crystal SANS diffractometer operating in combination with PSD.

## 2.4. High resolution small-angle neutron scattering

Small-angle neutron scattering investigations are carried out on the double-crystal diffractometer MAUD designed for the measurements in the high momentum transfer  $Q$ -resolution range. In contrast to conventional double-crystal arrangements, the fully asymmetric diffraction geometry on the elastically bent Si analyser is employed to transfer the angular distribution of the scattered neutrons



7. Powder diffraction spectrum from a Roman cavalry helmet.

FIG. 9. Photo of the analyser with the sample exchanger and 2d-position sensitive detector.

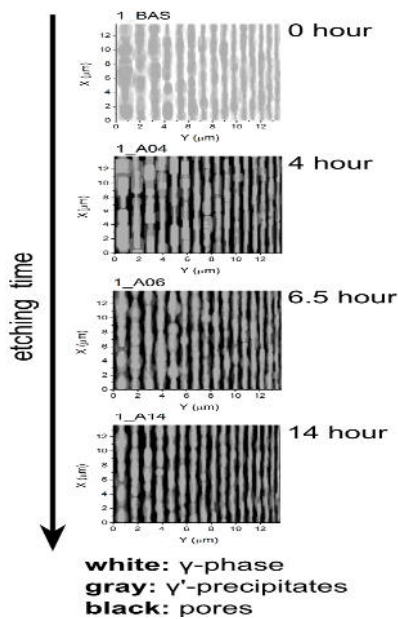


FIG. 10. Nanoporosity development in metallic membrane

to the spatial distribution and to analyse the whole scattering curve by a position sensitive detector (see Fig. 8) [16]. It reduces the exposure time per sample typically to 0.5-5 hours (depending on the

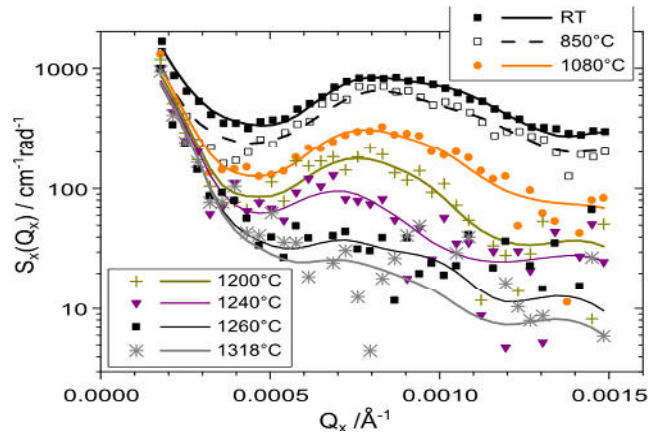


FIG. 11. Precipitate dissolution in CMSX4 single-crystal nickel-based superalloy

$Q$ -resolution and sample cross-section). Fig. 9 shows the photo of the analyser with the sample exchanger and 2d-position sensitive detector. The remote control of the curvatures of the monochromator and analyser crystals makes possible to tune the instrument resolution in the  $\Delta Q$  range from  $10^{-4}$  to  $10^{-3} \text{ \AA}^{-1}$ , according to the expected size of investigated inhomogeneities. An absolute calibration of scattering cross-sections is possible by measuring the intensity of the direct beam (no calibration samples are required). The instrument operates in fully automatic mode, including a sample exchange. The SANS diffractometer is in our case mainly used for studies of inhomogeneities in the size range from 50 nm to 1000 nm i.e. large precipitates in alloys (superalloys), porous materials (superplastic ceramics, ceramic thermal barrier coatings), nano-particles in ceramic-intermetallic compounds ( $\text{MoSi}_2$  with  $\text{Si}_3\text{N}_4$  and  $\text{SiC}$  particles) and large inhomogeneities in poly-mers/microemulsions (dimethyl-formamide-cyclohexan domains segregated by diblock copolymer). As application examples Fig. 10 and Fig. 11 show the results of studies of the nanoporosity in metallic membrane (where the aim of the experiment was to determine a dependence of the pore depth on the etching time by using SANS) and in-situ studies of high-temperature microstructure (precipitate dissolution in CMSX4 single-crystal nickel-based superalloy was investigated), respectively [17,18].

### Instrument parameters

Monochromator	bent perfect crystal Si(111), symmetric reflection
Sample	maximum irradiated cross-section $4 \times 25 \text{ mm}^2$
Analyser	bent perfect crystal Si 111, fully asymmetric geometry
Detector	2-dimensional position sensitive detector, $^3\text{He}$ filled, resolution $\sim 2 \text{ mm}$
Wavelength	$2.09 \text{ \AA}$
Neutron flux	$5 \times 10^3 \div 5 \times 10^4 \text{ n s}^{-1} \text{ cm}^{-2}$
Q-resolution	$10^{-4} \div 10^{-3} \text{ \AA}^{-1}$



Q-range	$2 \times 10^{-4} \div 2 \times 10^{-2} \text{ \AA}^{-1}$
Size range	500 $\text{\AA}$ - 2 micrometres

## 2.5. High resolution diffractometer for materials research

Two-axis high-resolution diffractometer optimized for investigation of elastic and plastic deformation studies in polycrystalline materials is installed at the channel HK9. The instrument is used especially for thermo-mechanical testing of materials, i.e. to study the deformation and transformation mechanisms of modern types of newly developed materials. Neutron diffraction performed in-situ upon external loads, brings a wide range of valuable structural and sub-structural parameters of the studied material which is easy to correlate with the parameters of external loads. The obtained microstructural parameters of the examined material can be directly compared with the parameters of micromechanical models. This approach brings a deeper understanding of processes ongoing in materials upon deformations, thermal treatments or phase transformations. The instrumental parameters are as follows: Horizontally and vertically focusing monochromator employing elastically bent Si single crystals, neutron wavelength  $1 \text{ \AA} \leq \lambda \leq 2.7 \text{ \AA}$ , neutron flux at the sample position  $10^5 \text{ n}\cdot\text{cm}^2\text{s}^{-1}$  at  $\lambda=2.3 \text{ \AA}$ , angular range of scattering angles  $25^\circ < 2\theta < 90^\circ$  and resolution  $2 \times 10^{-3} \leq \Delta d/d \leq 3 \times 10^{-3}$ . The following sample environments are at a disposal: Deformation machine for uni-axial loading (tension, compression)  $\pm 20 \text{ kN}$ , resistance heating ( $T < 1200^\circ\text{C}$ ) or hot-air heating ( $T < 300^\circ\text{C}$ ), miniature deformation machine for uni-axial loading (tension, compression)  $\pm 10 \text{ kN}$ , Eulerian cradle: inner diameter of 400 mm,  $0^\circ < \chi < 160^\circ$ ,  $0^\circ < \omega < 360^\circ$  and deformation machine for bending loading, maximum cycling frequency of 27 Hz. The neutron signal is recorded by 2-dimensional position sensitive detector. The above described methods have been recently mainly applied to the investigation of deformation mechanisms of magnesium alloys, including the innovative application of acoustic emission method simultaneously with neutron diffraction. Complementary dataset about the loading mode dependence of twinning was obtained, since acoustic emission is sensitive to twin nucleation whereas diffraction to twin growth. Theoretical calculations of Schmid-factor dependence of twin nucleation complete the experimental results which clearly explain the different behaviour of this material in tension and compression [19].

## 3. Summary

It has been demonstrated on a few examples that on the rather low power research reactor LVR-15 in Řež good quality experiments of basic, interdisciplinary as well as applied research can be effectively carried out. The research can cover a large scale of experimental investigations related to structure studies of new materials, structure phase transformations, chemistry, material testing, industrial product qualification, tracing of elements (e.g. in environmental, chemical, geological and biological samples), cultural heritage, etc. As the described instrumental development and measurements can be carried out at the low power neutron sources which require much lower safety requirements, in comparison with the medium and high flux neutron sources, they offer for students and young scientists excellent educational and training programmes in neutron scattering, nuclear analytical investigations with neutrons or imaging.

## Acknowledgement

The authors thank very much to colleagues from Neutron Physics Laboratory for providing related experimental results used in this paper. Measurements were carried out at the CANAM infrastructure of the NPI CAS Řež supported through MŠMT project No. LM2015056. The presented results were also supported in the frame of LM2015074 infrastructural MŠMT project Experimental nuclear reactors LVR-15 and LR-0.

## References

- [1] MIKULA, P., KYSELA, J., "Řež's Medium Power Research Reactor LVR-15 Opened for External Users", *Physics B*, **241-243** (1998) 39.
- [2] MIKULA, P., LUKÁŠ, P., STRUNZ, P., ŠAROUN, J., VRÁNA, M., DLOUHÁ, M., VRATISLAV, S., "Neutron Scattering Experiments of Materials Science at Řež's Reactor", *Physica B*, **241-243** (1998) 92.
- [3] VACÍK, J., HNATOWICZ, V., KÖSTER, U. "Diffusion of Boron in CaF<sub>2</sub>", *American Nuclear Society Transactions* **98** (2008) 422.
- [4] DOWNING, R.G., et al., "Neutron Depth Profiling: Overview and Description of NIST Facilities", *Journal of Research of NIST* **98** (1993) 109.
- [5] KUČERA, J., NOVÁK, J.K., KRANDA, K., PONCAR, J., KRAUSOVÁ, I., SOUKAL, L., CUNIN, O., LANG, M., "INAA and Petrological Study of Sandstones from the Angkor Monuments", *J. Radioanal Nucl. Chem.* **278** (2008) 299.
- [6] KUBEŠOVÁ, M., KUČERA J., "Validation of k<sub>0</sub> Standardization Method in Neutron Activation Analysis" (Proc. 5th Int k<sub>0</sub> Users Workshop, Belo Horizonte, Brazil, 2009).
- [7] ŘANDA, Z. et al., "Elemental characterization of the new Czech meteorite Morávka by neutron and photon activation analysis", *J. Radi. Nucl. Chem.*, **257** (2003) 275.
- [8] BISCHOFF, A. et al., "Jesenice—A new meteorite fall from Slovenia", *Meteorit. Planet. Sci.* **46** (2011) 793.
- [9] KRAUSOVÁ, I. et al., "Determination of <sup>129</sup>I in biomonitors collected in the vicinity of a nuclear power plant by neutron activation analysis", *J. Rad. Nucl. Chem.*, **295** (2013) 2043.
- [10] GALINHA, C. et al., "Selenium determination in cereal plants and cultivation soils by radiochemical neutron activation analysis", *J. Rad. Nucl. Chem.*, **294** (2012) 349.
- [11] GALINHA, C. et al., "Selenium in bread and durum wheats grown under a soil supplementation regime in actual field conditions, determined by cyclic and radiochemical neutron activation analysis", *J. Rad. Nucl. Chem.*, **304** (2015) 139.
- [12] KRAUSOVÁ, I. et al., "Impact of the brewing process on the concentration of silicon in lager beer", *J. Inst. Brew.*, **120** (2014) 433.
- [13] RASMUSSEN, K. L. et al., "Was he murdered or was he not?—Part I: Analyses of mercury in the remains of Tycho Brahe", *Archaeometry* **55** (2013) 1187.
- [14] WONG, C. H. A. et al., "Synthetic routes contaminate graphene materials with a whole spectrum of unanticipated metallic elements", *Proc. Nat. Acad. Sci. USA*, **111** (2014) 13774.
- [15] SMRČOK, L., PETRÍK, I., LANGER, V., FILINCHUK, Y., BERAN, P., "X-Ray, Synchrotron, and Neutron Diffraction Analysis of Roman Cavalry Parade Helmet Fragment" *Crystal Research and Technology* **45** (2010) No. 10, 1025.
- [16] STRUNZ, P., ŠAROUN, J., MIKULA, P., LUKÁŠ, P., EICHHORN, F., "Double Bent Crystal SANS Setting and its Applications", *J. Appl. Cryst.* **30** (1997) 844.
- [17] STRUNZ, P., MUKHERJI, D., NÄTH, O., GILLES, R., RÖSLER, J., "Characterization of Nanoporous Superalloy by SANS", *Physica B* **385-386** (2006) 626.
- [18] STRUNZ, P., MUKHERJI, D., ŠAROUN, J., KEIDERLING, U., RÖSLER, J., "Pore Structure Characterization and In-Situ Diffusion Test in Nanoporous Membrane Using SANS" *Journal of Physics: Conf. Series* **247** (2010) 012023.
- [19] ČAPEK, J., et al., "Study of the loading mode dependence of the twinning in random textured cast magnesium by acoustic emission and neutron diffraction methods", *Materials Science and Engineering A - Structural materials* **602** (2014) 25.